FUSION OF X RAY AND GEOMETRICAL DATA IN COMPUTED TOMOGRAPHY FOR NON DESTRUCTIVE TESTING APPLICATIONS

Ali Mohammad–Djafari
Laboratoire des Signaux et Systèmes (CNRS–SUPELEC–UPS)
École Supérieure d'Électricité
Plateau de Moulon, 91192 Gif–sur–Yvette Cedex, France.
E_mail: djafari@lss.supelec.fr

Abstract – *X ray computed tomography (CT) is widely used in non destructive testing (NDT) techniques. While in medical imaging, classical methods based on back projection (BP) or algebraic reconstruction techniques (ART) give satisfaction, in NDT applications, data acquiring constraints are such that these methods do not give satisfactory results. There is then a need for extra information and other kind of data. In this paper, we consider an X ray CT image reconstruction problem using two different kind of data: classical X-rays radiographic data and some geometrical informations and propose new methods based on regularization and Bayesian estimation approach for this data fusion problem. The geometrical information we use are of two kind: partial knowledge of values in some regions and partial knowledge of the edges of some other regions. We show the advantages of using such informations on increasing the quality of reconstructions in a NDT application of wide layered shape (sandwich) structures. We also show some results to analyze the effects of some errors in these data on the reconstruction results.*

Keywords: Computed tomography, Non destructive testing, Bayesian data fusion, Fusion of radiographic and geometric data.

1. INTRODUCTION

A widely used technique in industrial non destructive testing (NDT) application is X ray computed tomography (CT). While in medical imaging, classical methods based on back projection (BP) or algebraic reconstruction techniques (ART) give satisfaction, in NDT applications, data acquiring constraints (limited projection angles) are such that these methods do not give satisfactory results. Very often then, there is a need for extra information and other kind of data to obtain satisfactory results. Data fusion is then an active area of research in these applications. In this work, we consider the X ray CT image reconstruction problem using two different kind of data: classical radiographic (projection) data and some geometrical informations such as partial knowledge of materials in some regions and/or the borders of these or some other regions.

The idea of using geometrical data in CT imaging is not new. Many works on the subject has been done before. See for example [1, 2, 3, 4, 5, 6]. In [1], the authors proposed methods for using regions borders from geometrical data in medical imaging and the authors in [2, 3, 5, 6] used the knowledge of some of regions materials. While the application in the first reference concerns medical imaging, the application in the second references concerns industrial NDT. But, combining both regions and borders informations from anatomic data is new. We give here some preliminary results simulating a fan beam CT problem in NDT testing of metallic layer shaped media (sandwich structures) such as those of aircraft control surfaces. These structures are such that we cannot have a full range of projection data and the reconstruction problem is a strongly ill posed one due to limited-angle Radon transform null space. The authors in [3, 5] has also considered this problem, but the proposed method by these authors are based on projection on convex sets (POCS) which can not account for errors and extra knowledge as easily as in regularization or Bayesian estimation technique.

This paper is organized as follows: First, the basics of the Bayesian approach for heterogenous data fusion is presented. Then, we focus on the fusion of X ray and geometrical data and give details of the proposed method. Finally, we present a few simulated experiences showing comparisons of the results using classical back-projection or filtered back-projection methods with those obtained by the proposed method either using or not the geometric data. These results show the advantages of using geometric data when those data are exact and well registered with radiographic data. We also present some preliminary results showing the sensitivity of the proposed method to some errors in geometrical data due to imperfect registration and other uncertainties.

2. BAYESIAN APPROACH FOR DATA FUSION

Assume that we are observing an unknown quantity $\boldsymbol{x}$ through two different measurement systems and obtained two sets of data $\boldsymbol{y}$ and $\boldsymbol{z}$. For example, consider a NDT application and a CT imaging system where $\boldsymbol{x}$ represents the image of absorption coefficients of the object under the test, $\boldsymbol{y}$ a set of X ray radiographes and $\boldsymbol{z}$ a set of echo-graphic data obtained using a laser or an ultrasound probing system. The X ray data are related to the mass density $\boldsymbol{x}$ of the matter while the ultrasound data are related to the acoustic reflectivity $\boldsymbol{r}$ of the matter which is more related to the changes of material mass density inside the object and gives more information on the edges of different homogeneous regions.

One approach proposed and used by the author [7] and by other collaborators *Gautier et al.* [8, 6, 9] is based on a compound Markovian model where the body object $\boldsymbol{o}$ is assumed to be composed of three related quantities:

$$\boldsymbol{o} = \{\boldsymbol{x}, \boldsymbol{r}\} = \{\boldsymbol{x}, \boldsymbol{q}, \boldsymbol{a}\}$$

where $\boldsymbol{q}$ is a binary vector representing the positions of the discontinuities (edges) in the body, $\boldsymbol{a}$ a vector containing the reflectivity values such that when $q_j = 0$ then $r_j = 0$ and when $q_j = 1$ then $r_j = a_j$ and a_j. Note that, in principle, a_j must be related in some way to changes of density, *i.e.* $a_j = g(x_{j+1} - x_j)$, where g can be any monotonic increasing function. But, in practice, it is not easy to account for this dependence.

Using this model via a Bayesian estimation approach, we can write

$$p(\boldsymbol{o}) = p(\boldsymbol{x}, \boldsymbol{r}) = p(\boldsymbol{x}, \boldsymbol{a}, \boldsymbol{q}) = p(\boldsymbol{x}|\boldsymbol{a}, \boldsymbol{q})\, p(\boldsymbol{a}|\boldsymbol{q})\, p(\boldsymbol{q})$$

and using the Bayes rule, we have

$$\begin{aligned} p(\boldsymbol{x}, \boldsymbol{a}, \boldsymbol{q}|\boldsymbol{y}, \boldsymbol{z}) &\propto p(\boldsymbol{y}, \boldsymbol{z}|\boldsymbol{x}, \boldsymbol{a}, \boldsymbol{q})\, p(\boldsymbol{x}, \boldsymbol{a}, \boldsymbol{q}) \\ &= p(\boldsymbol{y}, \boldsymbol{z}|\boldsymbol{x}, \boldsymbol{a}, \boldsymbol{q}) p(\boldsymbol{x}|\boldsymbol{a}, \boldsymbol{q}) p(\boldsymbol{a}|\boldsymbol{q}) p(\boldsymbol{q}) \end{aligned}$$

To illustrate this approach more in details, let make the following assumptions:

• Conditional independence of $\boldsymbol{y}$ and $\boldsymbol{z}$:

$$p(\boldsymbol{y}, \boldsymbol{z}|\boldsymbol{x}, \boldsymbol{a}, \boldsymbol{q}) = p(\boldsymbol{y}|\boldsymbol{x})\, p(\boldsymbol{z}|\boldsymbol{a}, \boldsymbol{q}) = p(\boldsymbol{y}|\boldsymbol{x})\, p(\boldsymbol{z}|\boldsymbol{r}).$$

• Gaussian process for $\boldsymbol{\epsilon}_1$ and $\boldsymbol{\epsilon}_2$ which results to:

$$\begin{aligned} p(\boldsymbol{y}|\boldsymbol{x}; \sigma_1^2) &\propto \exp\left[-\tfrac{1}{2\sigma_1^2}||\boldsymbol{y} - \boldsymbol{H}_1\boldsymbol{x}||^2\right] \\ p(\boldsymbol{z}|\boldsymbol{r}; \sigma_2^2) &\propto \exp\left[-\tfrac{1}{2\sigma_2^2}||\boldsymbol{z} - \boldsymbol{H}_2\boldsymbol{r}||^2\right] \end{aligned}$$

• Bernoulli process for $\boldsymbol{q}$: $p(\boldsymbol{q}) \propto \sum_{i=1}^{n} q_i^{\lambda}(1 - q_i)^{1-\lambda}$

• Gaussian process for $\boldsymbol{r}|\boldsymbol{q}$ or equivalently for $\boldsymbol{a}|\boldsymbol{q}$:

$$p(\boldsymbol{a}|\boldsymbol{q}) \propto \exp\left[-\frac{1}{2\sigma_a^2}\boldsymbol{a}^t\boldsymbol{Q}\boldsymbol{a}\right], \boldsymbol{Q} = \text{diag}[q_1, \ldots, q_n]$$

• Independence of $\boldsymbol{x}$ and $\boldsymbol{a}$ and a Markovian model for $\boldsymbol{x}|\boldsymbol{q}$:

$$p(\boldsymbol{x}|\boldsymbol{a}, \boldsymbol{q}) = p(\boldsymbol{x}|\boldsymbol{q}) \propto \exp\left[-U(\boldsymbol{x}|\boldsymbol{q})\right]$$

Note that this hypothesis is not realistic, but it simplifies this introduction. Then, based on

$$p(\boldsymbol{x}, \boldsymbol{a}, \boldsymbol{q}|\boldsymbol{y}, \boldsymbol{z}) \propto p(\boldsymbol{y}|\boldsymbol{x})\, p(\boldsymbol{z}|\boldsymbol{a})\, p(\boldsymbol{x}|\boldsymbol{a}, \boldsymbol{q})\, p(\boldsymbol{a}|\boldsymbol{q})\, p(\boldsymbol{q})$$

many schemes can be proposed to estimate either $\boldsymbol{x}$ or both $(\boldsymbol{x}, \boldsymbol{r})$ or equivalently $(\boldsymbol{x}, \boldsymbol{a}, \boldsymbol{q})$:

• Simultaneous estimation of all the unknowns with the joint MAP estimation (JMAP):

$$(\widehat{\boldsymbol{x}}, \widehat{\boldsymbol{a}}, \widehat{\boldsymbol{q}}) = \arg \max_{(\boldsymbol{x}, \boldsymbol{a}, \boldsymbol{q})} \{p(\boldsymbol{x}, \boldsymbol{a}, \boldsymbol{q}|\boldsymbol{y}, \boldsymbol{z})\}$$

• First estimate $\boldsymbol{q}$ and $\boldsymbol{a}$ using only $\boldsymbol{z}$ and then use them to estimate $\boldsymbol{x}$:

$$\begin{cases} (\widehat{\boldsymbol{q}}, \widehat{\boldsymbol{a}}) = \arg \max_{\boldsymbol{q}, \boldsymbol{a}} \{p(\boldsymbol{q}, \boldsymbol{a}|\boldsymbol{z})\} \\ \widehat{\boldsymbol{x}} = \arg \max_{\boldsymbol{x}} \{p(\boldsymbol{x}|\boldsymbol{y}, \widehat{\boldsymbol{a}}, \widehat{\boldsymbol{q}})\} \end{cases}$$

• First estimate only $\boldsymbol{q}$ using $\boldsymbol{z}$ and then estimate $\boldsymbol{x}$ using $\widehat{\boldsymbol{q}}$ and the data $\boldsymbol{y}$:

$$\begin{cases} \widehat{\boldsymbol{q}} &= \arg \max_{\boldsymbol{q}} \{p(\boldsymbol{q}|\boldsymbol{z})\} \\ \widehat{\boldsymbol{x}} &= \arg \max_{\boldsymbol{x}} \{p(\boldsymbol{x}|\boldsymbol{y}, \widehat{\boldsymbol{q}})\} \end{cases}$$

Other schemes are possible [7]. In all these schemes, the detection steps (estimation of $\boldsymbol{q}$) is very difficult and computationally demanding due to the need of marginalization and a combinatorial optimization algorithm. One way to take over this difficulty is to model the object only by $(\boldsymbol{r}, \boldsymbol{x})$ without decomposing $\boldsymbol{r}$ in $(\boldsymbol{q}, \boldsymbol{a})$ anymore. However, we must catch the pulse shape information of $\boldsymbol{r}$ (r_j is almost always equal to zero in homogeneous regions and can take any real value in the borders of these regions). This can be done through a better choice for $p(\boldsymbol{r})$. For example, a generalized Gaussian law for $p(\boldsymbol{r})$:

$$p(\boldsymbol{r}) \propto \exp\left[-\alpha \sum_j |r_j|^{\beta}\right] \quad \text{with} \quad 1 \leq \beta \leq 2,$$

in place of Gaussian law which is the special case for $\beta = 2$. This choice, thanks to long-tailed character of this distribution for the values of β near to one, gives the possibility to account for the concentration around zero of the histogram of the values of r_j while giving the possibility to have large values.

Based on this remark, a more realistic solutions has been proposed in previous works [10, 9, 7, 11] which is described briefly through the following scheme:

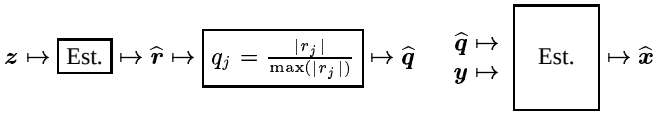

For the first part, with the assumptions made, we have

$$\widehat{\boldsymbol{r}} = \arg\max_{\boldsymbol{r}} \{p(\boldsymbol{r}|\boldsymbol{z})\} = \arg\min_{\boldsymbol{r}} \{J_1(\boldsymbol{r}|\boldsymbol{z})\}$$

with

$$J_1(\boldsymbol{r}|\boldsymbol{z}) = ||\boldsymbol{z} - \boldsymbol{H}_2\boldsymbol{r}||^2 + \lambda \sum_j |r_j|^\beta.$$

When $\boldsymbol{r}$ estimated, we can determine either a binary valued $\boldsymbol{q}$ from it by using a threshold value s ($q_j = 1$, if $|r_j| < s$ and $q_j = 0$ elsewhere), or a real valued $\boldsymbol{q}$ with $q_j \in [0, 1]$ by $q_j = |r_j| / \max(|r_j|)$ or any other practical solution. This real valued $\boldsymbol{q}$ can be considered as a blurred (or fuzzy) image of borders and edges.

For the second part which is the estimation of $\boldsymbol{x}$ given $\boldsymbol{y}$ and $\widehat{\boldsymbol{q}}$ the following criterion has been used:

$$\widehat{\boldsymbol{x}} = \arg\max_{\boldsymbol{x}} \{p(\boldsymbol{x}|\boldsymbol{y}, \widehat{\boldsymbol{q}})\} = \arg\min_{\boldsymbol{x}} \{J_2(\boldsymbol{x}|\boldsymbol{y}; \widehat{\boldsymbol{q}})\}$$

with

$$J_2(\boldsymbol{x}|\boldsymbol{y}, \widehat{\boldsymbol{q}}) = ||\boldsymbol{y} - \boldsymbol{H}_1\boldsymbol{x}||^2 + \lambda_2 \sum_j (1 - q_j)|x_{j+1} - x_j|^\beta, \quad 1 \leq \beta \leq 2.$$

3. FUSION OF GEOMETRIC INFORMATION AND RADIOGRAPHIC DATA

Here, we illustrate an application of the proposed method for the special case of limited angle CT imaging where we want to include some geometric information, such as partial knowledge of borders of different regions and/or partial knowledge of materials in specified regions of the body in the reconstruction method.

Using some partial knowledge of some regions borders can be considered as a special case of the previous example. Actually, in the second step of the proposed method in previous section, we were using the combination of the radiographic data $\boldsymbol{y}$ and $\boldsymbol{q}$ which can be considered as a geometrical (regions borders) data. Here we propose to add a new term to this criterion to include some partial knowledge about the values of pixels in some specified regions. Because this information may be partial and there may also be some uncertainty on it, we use again probabilistic approach and model this through a probability law

$$p(\boldsymbol{x}|\boldsymbol{s}) \propto \exp\left[-\mu_j |x_j - s_j|^{\beta_2}\right]$$

where $\boldsymbol{s}$ is an image containing the attenuation constant values of some of the regions in the body (not forcibly the same regions for which we know the borders) and $\boldsymbol{\mu}$ an image indicating our degree of confidence about the knowledge of values in those regions (0 when no knowledge and 1 when high confidence). Using this model and the discussions in previous sections, the Bayesian MAP estimation approach comes up with the following criterion to optimize to find the an image $\widehat{\boldsymbol{x}}$ which will be the result of fusion of these data:

$$\begin{aligned} J(\boldsymbol{x}|\boldsymbol{y}, \boldsymbol{q}, \boldsymbol{s}, \boldsymbol{\mu}) = & ||\boldsymbol{y} - \boldsymbol{H}_1\boldsymbol{x}||^2 \\ & + \lambda_1 \textstyle\sum_j (1 - q_j)|x_{j+1} - x_j|^{\beta_1} \\ & + \lambda_2 \textstyle\sum_j \mu_j |x_j - s_j|^{\beta_2} \end{aligned} \quad (1)$$

Note that, when the hyperparameters $\lambda_1, \lambda_2 > 0$ and $1 \leq \beta_1, \beta_2 \leq 2$ and the data $\boldsymbol{y}$ and $\boldsymbol{q}, \boldsymbol{s}$ and $\boldsymbol{\mu}$ are given, this criterion is a convex function of $\boldsymbol{x}$. Then, its optimization can be done by any gradient based algorithm. In the following, we show the results obtained by this criterion for the following situations:
– when we do not have any geometrical data ($\boldsymbol{q} = \boldsymbol{\mu} = \boldsymbol{0}$);
– when we have only the map of borders $\boldsymbol{q}$ but no region data ($\boldsymbol{\mu} = \boldsymbol{0}$);
– when we have only the map of regions (characterized by both $\boldsymbol{s}$ and $\boldsymbol{\mu}$) but no other borders data ($\boldsymbol{q} = \boldsymbol{0}$);
– when we have both the borders $\boldsymbol{q}$ and regions maps $(\boldsymbol{s}, \boldsymbol{\mu})$.
– when we have both the borders $\boldsymbol{q}$ and regions maps $(\boldsymbol{s}, \boldsymbol{\mu})$ but with some errors in those data to measure the sensitivity of the results to those errors.

In the following, the hyperparameters β_1 and β_2 are fixed either to 2 or to 1.1 and the two regularization parameters λ_1 and λ_2 are adjusted empirically.

We have recently tested the same proposed method in a medical imaging with a fan-beam geometry where we used anatomical data as complementary data.

A final remark concerns the adaptation of the criterion to 2D case where we may distinguish between horizontal, vertical and diagonal edges. In that case we may replace the second term $\lambda_1 \sum_j (1-q_j)|x_{j+1} - x_j|^{\beta_1}$ of the criterion (1) by the following:

$$\begin{aligned} & \lambda_h \sum_{i=1}^{M} \sum_{j=1}^{N-1} (1 - h_{ij})|x_{i,j+1} - x_{i,j}|^{\beta_1} + \\ & \lambda_v \sum_{i=1}^{M-1} \sum_{j=1}^{N} (1 - v_{ij})|x_{i+1,j} - x_{i+1,j}|^{\beta_1} + \\ & \lambda_{hv} \sum_{i=1}^{M-1} \sum_{j=1}^{N-1} (1 - qv_{ij})|x_{i+1,j+1} - x_{i,j}|^{\beta_1} + \\ & \lambda_{vh} \sum_{i=1}^{M-1} \sum_{j=2}^{N} (1 - vq_{ij})|x_{i+1,j-1} - x_{i,j}|^{\beta_1}, \end{aligned}$$

where h_{ij}, v_{ij}, qv_{ij} and vq_{ij} are, respectively, horizontal, vertical, first diagonal and second diagonal map edges. The corresponding parameters λ_h, λ_v, λ_{hv} and λ_{vh} give the possibility to balance their relative uncertainties.

4. SIMULATION EXPERIMENTS

The application concerned here is non destructive testing (NDT) of composite wide sandwich structures where we

may have very limited angle projections. The reconstruction problem is then more ill conditioned than the case of where we can turn around the object under the test as is the case in medical imaging.

Here, we simulated a case where we can only position the X ray source in a very limited number of points on the upper side of the object under the test and simulated a fan-beam geometry, where for each position of the source, an array of 256 CCD element, in a fixed position at the lower side of the object, measures the amplitude of attenuated rays. Figure 1 shows this configuration.

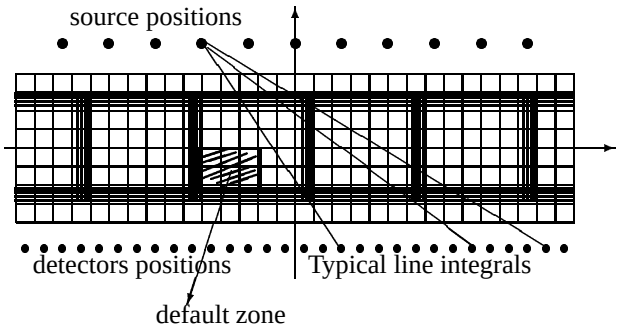

Fig. 1. Geometrical configuration of the NDT of wide sandwich structures via X ray computed tomography.

We assume then that we know or we can measure the outside profile of the object using a pulse-echo technique using either ultrasound or a laser beam. Thus, we may know the exact outside profile and the thickness of the two external layers. Figure 2 shows this pulse-echo external profile measurement configuration.

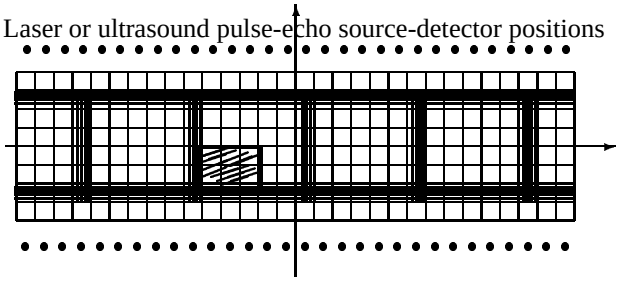

Fig. 2. Laser or ultrasound pulse-echo external profile measurement configuration.

Figure 3 shows the original object and the associated sinogram data.

Figure 4 shows the reconstruction results by classical back-projection or filtered back-projection methods used in commercial scanners. As it is seen on this figure, these results are not satisfactory for the data gathering configuration we proposed where we are looking for a high resolution image (64×256) from a sinogram data which has only (11×256) data points (256 detectors and 11 source positions). We also give here two other results obtained by optimizing the criterion

$$J(\boldsymbol{x}|\boldsymbol{y},\boldsymbol{q},\boldsymbol{s}) = ||\boldsymbol{y} - \boldsymbol{H}_1\boldsymbol{x}||^2 + \lambda_1 \sum_j (x_{j+1} - x_j)^2$$

once over $\mathbf{R}^n$ and the second over $\mathbf{R}^n_+$. In both cases, we used a simple gradient algorithm, but in the second case, we imposed the positivity constraint at each iteration. These results are significantly better than the classical back-projection methods thanks to regularization terms, but they need more computations (approximately two times more computations than a simple back-projection in each iteration).

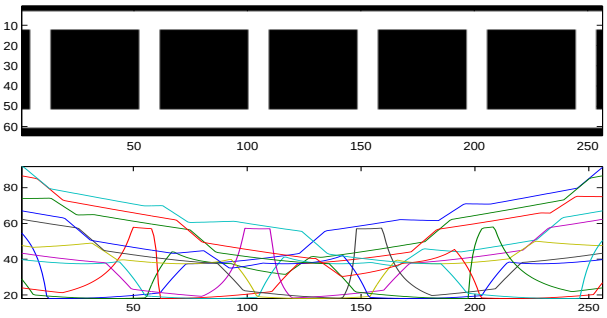

Fig. 3. Original object (top) and the eleven projection data each corresponding to one source position (bottom). The geometry is a fan beam CT, the object space is discretized to (64×256) pixels and the sinogram data has (11×256) data points (11 X-ray source position and 256 CCD sensors).

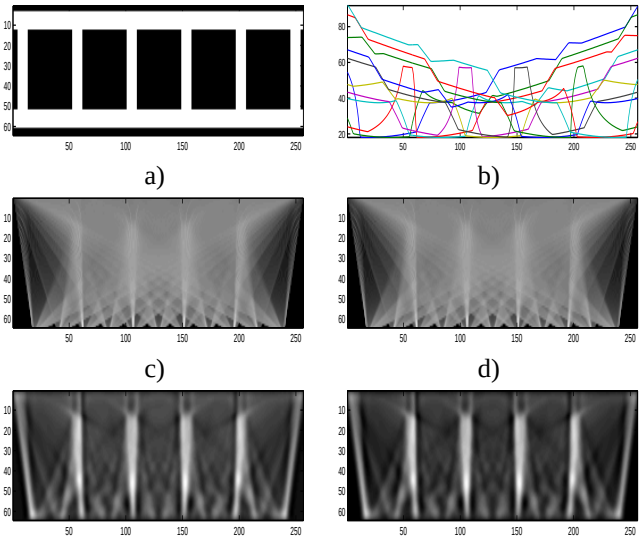

Fig. 4. Reconstructions by classical methods:
a) original object, b) projection data;
c) back-projection, d) filtered back-projection;
e) quadratic regularization and f) quadratic regularization with positivity constraint.

Figure 5 shows the reconstruction results using geometrical data. In this figure, a) and b) show the known region and borders data which are assumed available; c) shows the result when only the region data in a) has been used; d) shows the result when only the borders data in b) has been used; and e) and f) are two results when both region and borders data have been used. These two results have been obtained for two different values of confidence for the regions values (different values of λ_2 which is too low at left but it seems to have good value at right.

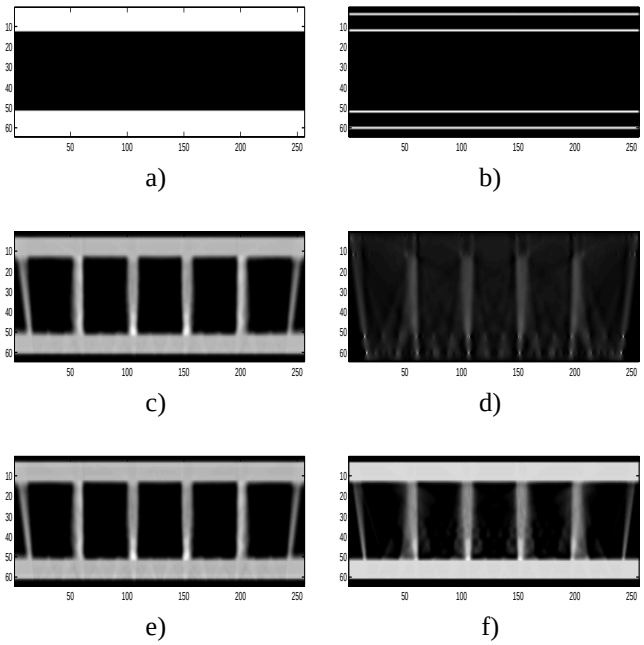

Fig. 5. Reconstructions by data fusion with exact geometrical data:
a) known regions data, b) known borders data;
c) Results using a), d) Results using b);
e) and f) Results using both a) and b) for two different values of confidence for the regions values (different values of λ_2 which is too low at left but it seems to have good value at right).

Obviously, fusion of more geometrical information results in more accurate results when the geometrical results are exact. From these numerical experiments, we also see that borders and edges information brings less information than the region values. This can be seen when comparing the results using only borders and edges (5.c) or only region values informations (5.d).

However, in practical applications, we need a first step of registration to bring the geometrical informations in the same frames of X ray radiographic data. In previous simulations, we assumed that this has been done, before starting the reconstruction.

In the following, we give some results to show the sensitivity of the results on some errors on the geometrical data. Here, we simulated the case where there is an error of about 12.5% on the thickness of the two external layers (1 pixel over 8).

Figure 6 shows the results obtained with these errors in the geometrical data with the same conditions which are obtained the results of the figure 3.

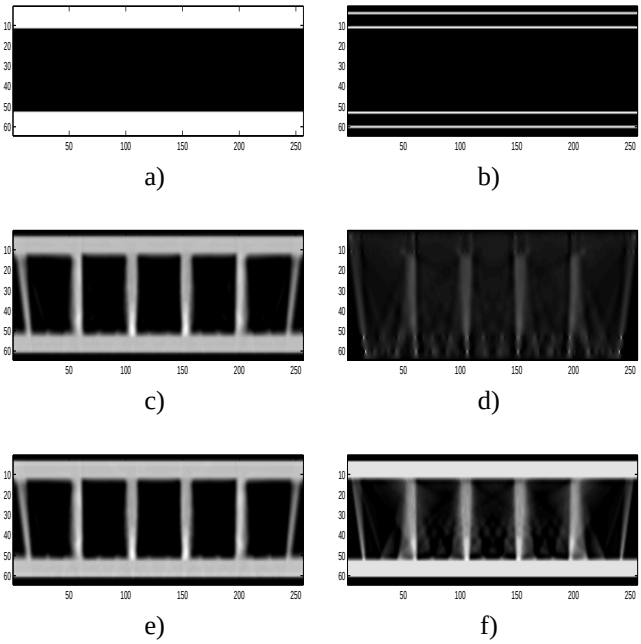

Fig. 6. Reconstructions by data fusion with errors in the geometrical data:
a) known regions with errors, b) known borders with errors;
c) result using a), d) result using b);
e) and f) results using both a) and b) for two different values of confidence for the regions values. These results are to be compared with those of Fig. 5 which were obtained with exact geometrical data.

Comparing these results, we see that the degradations due to these errors are not so crucial if the regularization parameters λ_1 and λ_2 are not too high. We can also remark that, errors on edges are less important than the errors on the region values. This can be understand, because, the information content of the region values are higher than the edges and borders.

There is however the possibilities to reduce these effects, by feedback iterating, i.e. by reestimating these geometrical data from the final reconstructions of the previous results and restarting the data fusion again from these new informations and we are working on it and probably we will present the results in the final paper. However, nothing can prove the convergence of such an iterative procedure.

In Fig. 7 we present the results for the same object with an additional default region inside the layered region to show the capability of the proposed method to detect such defaults.

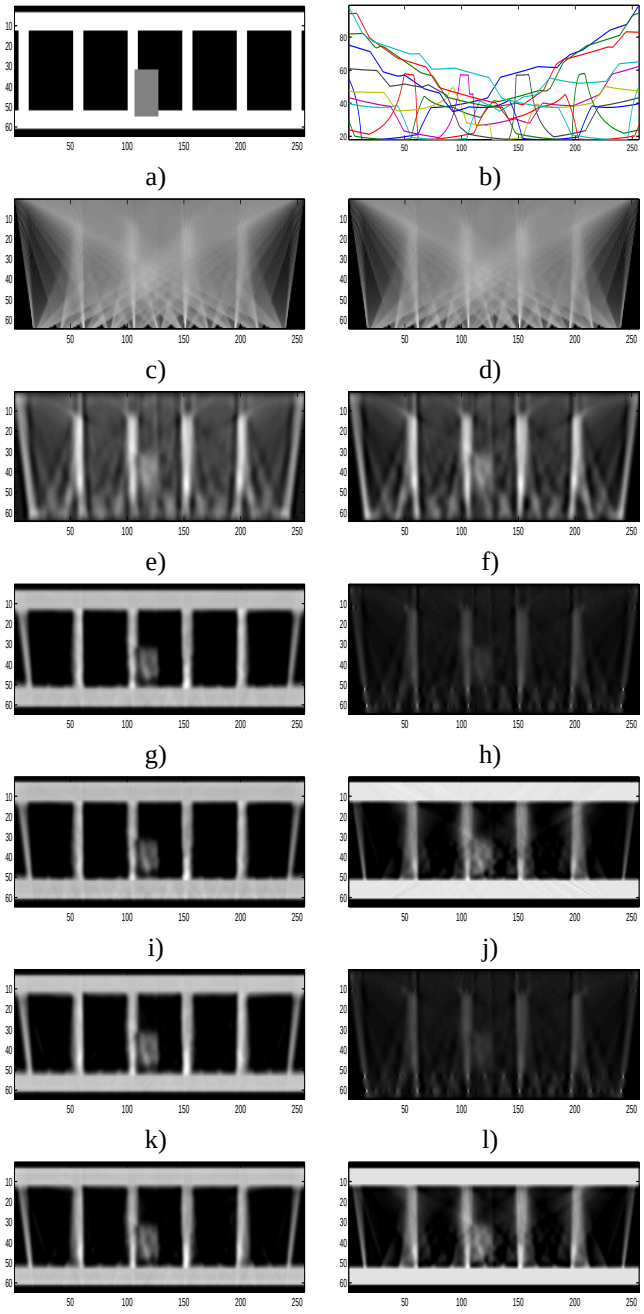

Fig. 7. Reconstructions results for an object with default area: a) Object with default area, b) 11 projection data; c) back-projection, d) filtered back-projection; e) quadratic regularization and f) quadratic regularization with positivity constraint; g) Results using known regions and h) Results using known borders; i) and j) Results using both regions and borders data for two different values of confidence for the regions values; k), l), m) and n) are the results equivalent to g), h) ,i) and j) but with errors in geometrical data.

Finally, in Fig. 8, we present the same results as in Fig.7, but for a more favorable situation where we have more data (21 X ray projection data in place of 11). We can see that the reconstruction results are much better than those in Fig. 7.

5. FUTURE WORKS

We propose the following extensions to this work:

- The first is to replace the binary valued map of borders $\boldsymbol{q}$ by a real valued $q_j \in [0,1]$ which will result to a more robust criterion against the errors in this map.

- The second is to extend this work in 3D case.

- The third and more important is to replace the criterion (1) by a more general one

$$\begin{aligned} J(\boldsymbol{x}|\boldsymbol{y},\boldsymbol{q},\boldsymbol{s},\boldsymbol{\mu}) = & ||\boldsymbol{y}-\boldsymbol{H}_1\boldsymbol{x}||^2 \\ & + \lambda_1 \textstyle\sum_j (1-q_j)\phi_1(x_{j+1}-x_j) \\ & + \lambda_2 \textstyle\sum_j \mu_j \phi_2(x_j - s_j) \\ & + \lambda_3 \textstyle\sum_j |x_j|^2 \end{aligned} \tag{2}$$

where the third term can be of help for the cases where the images we are looking for has great homogeneous low absorption materials (air), and ϕ_1 and ϕ_2 can have other expressions than a quadratic or power form. We think in particular to all the potential functional forms with edge preserving properties such as

$$\phi(u) = \{2\ln(cosh(u)), \quad 2\sqrt{1+u^2}-2\}$$

which are convene [12, 13], or

$$\phi(u) = \{\min(u^2,1), \quad u^2/(1+u^2), \quad \ln(1+u^2)\}$$

which are non convene [14, 15, 16]. The main advantage of doing this is to use half-quadratic optimization algorithms [17, 18, 19, 20] and having explicit expression for estimating edges when the solution is computed. This will give us the possibility to estimate $\widehat{\boldsymbol{q}}$ from $\widehat{\boldsymbol{x}}$, replace some of the values of it by known values of $\boldsymbol{q}$ and use it again in the next iteration. The whole reconstruction procedure will be the following:
1. Initialize $\boldsymbol{q} = \boldsymbol{q}^{(0)}$;
2. Compute $\boldsymbol{x}$ by optimizing the criterion (2);
3. Compute a new value for $\boldsymbol{q}$ from $\boldsymbol{x}$ using the properties of half-quadratic criteria;
4. Replace those a priori known values of values of $\boldsymbol{q}^{(0)}$ in computed $\boldsymbol{q}$ and return to 2 until convergence.

We may report some of these results in the final paper.

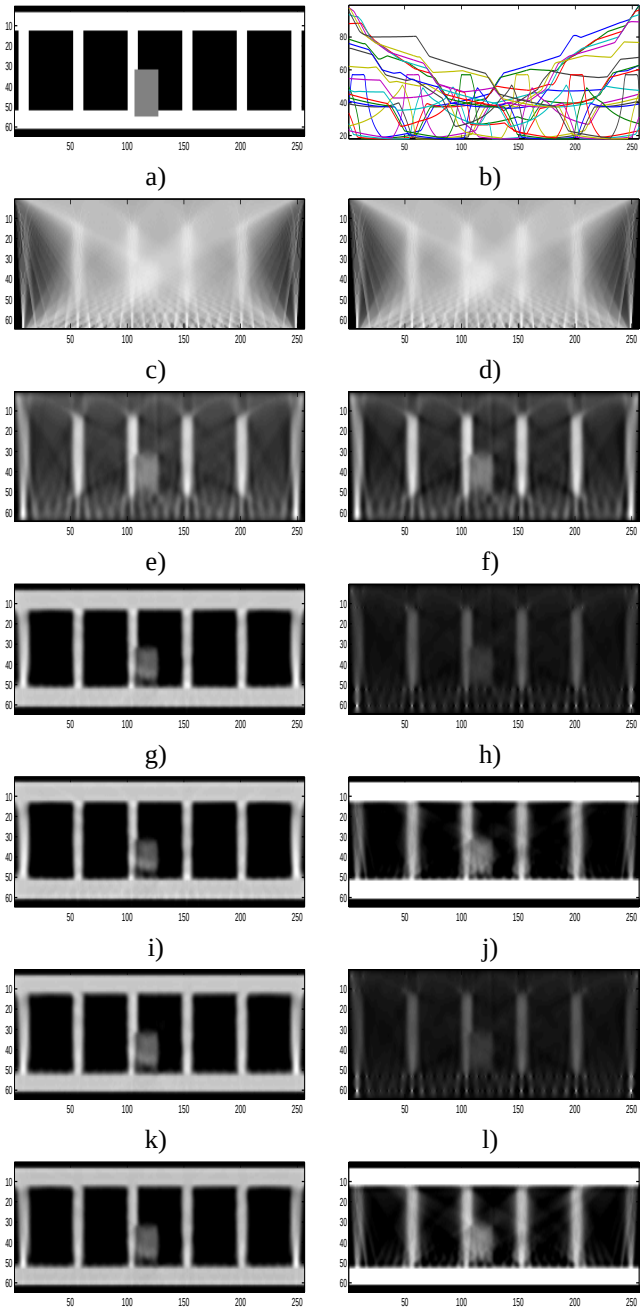

Fig. 8. Reconstructions results for an object with default area: a) Object with default area, b) 21 projection data; c) back-projection, d) filtered back-projection; e) quadratic regularization and f) quadratic regularization with positivity constraint; g) Results using known regions and h) Results using known borders; i) and j) Results using both regions and borders data for two different values of confidence for the regions values; k), l), m) and n) are the results equivalent to g), h) ,i) and j) but with errors in geometrical data. These results are to be compared with those of Fig. 7. with less X ray data (11 in Fig. 7 and 21 here).

6. CONCLUSIONS

We illustrated the feasibility of a Bayesian estimation approach for data fusion in a NDT application using computed tomography where we used some geometrical information to obtain better reconstruction results. We used two kind of geometrical information: partial knowledge of values in some regions and/or partial knowledge of the borders of some other regions. We showed the advantages of using such informations on increasing the quality of reconstructions. We also showed some results to analyze the effects of some errors in anatomic data on the reconstructed results.

7. REFERENCES

[1] G. Gindi, M. Lee, A. Rangarajan, and I. G. Zubal, "Bayesian reconstruction of functional images using anatomical information as priors," *IEEE Trans. Medical Imaging*, vol. MI-12, no. 4, pp. 670–680, 1993.

[2] M. Fiani, J. Idier, and S. Gautier, "Algorithmes ART semi-quadratiques pour la reconstruction à partir de radiographies," in *Actes du 18e colloque GRETSI*, Toulouse, Sept. 2001.

[3] J. Boyd and J. Little, "Complementary data fusion for limited-angle tomography," in *Proceeding of Computer Vision and Pattern Recognition 1994*, Seattle, WA, USA, 1994, pp. 288–294.

[4] G. Matsopoulos, S. Marshall, and J. Brunt, "Multiresolution morphological fusion of mr and ct images of the human brain," *IEE Proceedings on Vision, Image and Signal Processing*, vol. 141 Issue: 3, pp. 137 – 142, 1994.

[5] J. Boyd, "Limited-angle computed tomography for sandwich structures using data fusion," *Journal of Nondestructive Evaluation*, vol. 14, no. 2, pp. 61–76, 1995.

[6] S. Gautier, G. Le Besnerais, A. Mohammad-Djafari, and B. Lavayssière, "Fusion de données radiographiques et ultrasonores, en vue d'une applicaion en contrôle non destructif," Clermont-Ferrand, May 1995, Second international workshop on inverse problems in electromagnetism and acoustic.

[7] A. Mohammad-Djafari, "Probabilistic methods for data fusion," in *Maximum Entropy and Bayesian Methods*, Boise, ID, Aug. 1997.

[8] S. Gautier, G. Le Besnerais, A. Mohammad-Djafari, and B. Lavayssière, *Data fusion in the field of non destructive testing*, Maximum Entropy and Bayesian Methods. Kluwer Academic Publ., Santa Fe, NM, K. Hanson edition, 1995.

[9] S. Gautier, *Fusion de données gammagraphiques et ultrasonores. Application au contrôle non destructif*, Phd thesis, Université de Paris-Sud, Orsay, Dec. 1996.

[10] S. Gautier, G. Le Besnerais, A. Mohammad-Djafari, and B. Lavayssière, "Vers la fusion de données gammagraphiques et ultrasonores," in *Actes du 15*e *colloque GRETSI*, Juan-les-Pins, Sept. 1995, pp. 869–872.

[11] S. Gautier, J. Idier, A. Mohammad-Djafari, and B. Lavayssière, "X-ray and ultrasound data fusion," in *Proc. IEEE ICIP*, Chicago, IL, Oct. 1998, pp. 366–369.

[12] P. J. Green, "Bayesian reconstructions from emission tomography data using a modified EM algorithm," *IEEE Trans. Medical Imaging*, vol. MI-9, no. 1, pp. 84–93, Mar. 1990.

[13] P. Charbonnier, L. Blanc-Féraud, G. Aubert, and M. Barlaud, "Two deterministic half-quadratic regularization algorithms for computed imaging," in *Proc. IEEE ICIP*, Austin, TX, USA, Nov. 1994, vol. 2, pp. 168–172.

[14] A. Blake and A. Zisserman, *Visual reconstruction*, The MIT Press, Cambridge, 1987.

[15] T. Hebert and R. Leahy, "A generalized EM algorithm for 3-D Bayesian reconstruction from Poisson data using Gibbs priors," *IEEE Trans. Medical Imaging*, vol. 8, no. 2, pp. 194–202, June 1989.

[16] D. Geman and G. Reynolds, "Constrained restoration and the recovery of discontinuities," *IEEE Trans. Pattern Anal. Mach. Intell.*, vol. 14, no. 3, pp. 367–383, Mar. 1992.

[17] D. Geman and C. Yang, "Nonlinear image recovery with half-quadratic regularization," *IEEE Trans. Image Processing*, vol. 4, no. 7, pp. 932–946, July 1995.

[18] G. Aubert and L. Vese, "A variational method in image recovery," *SIAM J. Num. Anal.*, vol. 34, no. 5, pp. 1948–1979, Oct. 1997.

[19] P. Charbonnier, L. Blanc-Féraud, G. Aubert, and M. Barlaud, "Deterministic edge-preserving regularization in computed imaging," *IEEE Trans. Image Processing*, vol. 6, no. 2, pp. 298–311, Feb. 1997.

[20] J. Idier, Y. Goussard, and A. Ridolfi, "Unsupervised image segmentation using a telegraph parameterization of Pickard random fields," in *Spatial statistics. Methodological aspects and some applications*, M. Moore, Ed., vol. 159 of *Lecture notes in Statistics*, pp. 115–140. Springer Verlag, New York, NY, 2001.